

Investigation of motor unit recruitment during stimulated contractions of tibialis anterior muscle

*Original*

Investigation of motor unit recruitment during stimulated contractions of tibialis anterior muscle / Mesin, Luca; Merlo, Enrico; Merletti, Roberto; Orizio, C.. - In: JOURNAL OF ELECTROMYOGRAPHY AND KINESIOLOGY. - ISSN 1050-6411. - STAMPA. - 20:4(2010), pp. 580-589. [10.1016/j.jelekin.2009.11.008]

*Availability:*

This version is available at: 11583/2290697 since:

*Publisher:*

Elsevier

*Published*

DOI:10.1016/j.jelekin.2009.11.008

*Terms of use:*

This article is made available under terms and conditions as specified in the corresponding bibliographic description in the repository

*Publisher copyright*

(Article begins on next page)

5

# Investigation of motor unit recruitment during stimulated contractions of tibialis anterior muscle

Mesin L.<sup>1</sup>, Merlo E.<sup>1,2</sup>, Merletti R.<sup>1</sup>, Orizio C.<sup>2</sup>

10

<sup>1</sup> *Laboratorio di Ingegneria del Sistema Neuromuscolare e della Riabilitazione Motoria (LISiN),*

*Dipartimento di Elettronica, Politecnico di Torino, Torino, Italy.*

<sup>2</sup> *Dipartimento Scienze Biomediche e Biotecnologie, Università degli Studi di Brescia, Brescia, Italy*

15

**Running title:** MU electromechanical responses to transcutaneous electrical stimulation.

20

**Corresponding author:**

Roberto Merletti, LISiN

Dipartimento di Elettronica, Politecnico di Torino; Corso Duca degli Abruzzi 24, Torino, 10129 ITALY

Tel. 0039-011-4330476; Fax. 0039-011-4330404; e-mail : roberto.merletti@polito.it

25

**ABSTRACT**

This work investigated motor unit (MU) recruitment during transcutaneous electrical stimulation (TES) of the tibialis anterior (TA) muscle, using experimental and simulated data. Surface electromyogram (EMG) and torque were measured during electrically-elicited contractions at 5 different current intensities, on eight healthy subjects.

EMG detected during stimulation (M-wave) was simulated selecting the elicited MUs on the basis of: a) the simulated current density distribution in the territory of each MU and b) the excitation threshold characteristic of the MU. Exerted force was simulated by adding the contribution of each of the elicited MUs. The effects of different fat layer thickness (between 2 and 8 mm), different 10 distributions of excitation thresholds (random excitation threshold, higher threshold for larger MUs or smaller MUs), and different MU distributions within the muscle (random distribution, larger MU deeper in the muscle, smaller MU deeper) on EMG variables and torque were tested.

Increase of the current intensity led to a first rapid increase of experimental M-wave amplitude, followed by a plateau. Further increases of the stimulation current determined an increase of the 15 exerted force, without relevant changes of the M-wave. Similar results were obtained in simulations.

Rate of change of conduction velocity (CV) and leading coefficient of the second order polynomial interpolating the force vs stimulation level curve were estimated as a function of increasing current amplitudes. Experimental data showed an increase of estimated CV with increasing levels of the stimulation current (for all subjects) and a positive leading coefficient of force vs stimulation 20 current curve (for 5 out of 8 subjects). Simulations matched the experimental results only when larger MUs were preferably located deeper in the TA muscle (in line with a histochemical study).

Marginal effect of MU threshold was observed, suggesting that MUs closer to the stimulation electrode are recruited first during TES regardless of their excitability thresholds.

**Keywords:** Motor unit recruitment, motor unit distribution, electrical stimulation, M-wave, 25 modeling, EMG.

## 1. INTRODUCTION

Electrical stimulation (ES) of the peripheral nervous system is attracting increasing attention because of its wide range of applications aimed to investigate or improve muscle function (in physiological conditions as well as during fatiguing contractions or in the case of neuromuscular disorders). In particular, electrically evoked muscle contractions have been used as a tool to prevent disuse and/or denervation atrophy (Dimitrijevic and Dimitrijevic, 2002), to improve voluntary control in stroke patients (Sadowsky, 2001), to reduce spasticity (Skold et al 2002), to achieve functional control of paralyzed extremities (Bajd et al 1999) (functional electrical stimulation - FES) and to monitor muscle function changes due to exposure to microgravity and to evaluate the effectiveness of countermeasures (Mayr et al 1999).

Transcutaneous ES (TES) is a specific type of muscle stimulation (Merletti et al 1990; Orizio et al 2004). When delivered at the muscle motor point, it is well tolerated by the subject. A deeper insight into the mechanisms by which the delivered current pulse induces the activation of the muscle fibers (recruitment pattern) belonging to the considered motor point is crucial for optimal exploitation of TES in clinical practice. A progressively increasing stimulation current density flowing through axons of different sizes activates those with larger diameter first (Gorman and Mortimer 1983; Solomonow et al 1986). During TES, it seems that the synchronous activation of muscle fibers is achieved by stimulating the motoneuron terminal branches (Merletti et al 1990). As the current density induced by TES varies point by point in the tissues (decaying rapidly with depth, Mesin and Merletti 2008), the recruitment of the motor units (MU) is not only influenced by the diameter of the axonal branches (possibly not correlated to the diameter of the parent motoneuron axon), but also by geometric factors (location of the MUs and orientation of the terminal branches with respect to the current flow, Merletti et al 1990).

To study MU recruitment during TES, the characteristics of the evoked electrical and mechanical activity of the recruited muscle fibers may be investigated. Surface electromyogram (EMG) detected during TES (M-wave) is the summation of the electrical contributions of the recruited

MUs. Its amplitude and its conduction velocity (CV) are influenced by factors such as: number and type of the elicited MUs, position of the neuromuscular junctions, MU distribution within the muscle (random or large near the surface, small in the core or vice versa), thickness and conductivity of the subcutaneous tissues, position and orientation of the detection system (Farina et al 2004b). Because of these many factors affecting the muscle electrical response and because of their different weight in different muscles and subjects, it is not surprising that several studies using variables extracted from M-waves to monitor the recruitment order during TES gave controversial results, suggesting either the recruitment from larger to smaller MUs (Heyters et al 1994; Trimble and Enoka 1991) or just the opposite (Feiereisen et al 1997; Knaflitz et al 1990). The mechanical response to ES provides additional information which doesn't depend on many of the factors affecting the M-wave (e.g., MU location within the muscle and tissue geometry and conductivity). Thus, joint recording of electrical and mechanical responses helps to investigate the physiology of TES.

To investigate the recruitment of MUs during TES, a fruitful approach is the simulation of the current density distribution induced within the muscle by the external stimulation. A previous work (Farina et al 2004a) analyzed MU activation order with increasing transcutaneous electrical stimulation by comparing experimental and simulated signals. Only the electrical response was investigated. It was suggested that MUs in biceps brachii were recruited from low to high CV (small to large fibers MUs) and from superficial to deep muscle layers. The current density field within the muscle was not simulated in (Farina et al 2004a), so the recruitment of MUs was assumed in a particular order, without the support of a structure based model of electrical stimulation. Another work provided a model of electrical stimulation (Kuhn et al 2009), but only the mechanical response was investigated.

This work investigates the mechanism underlying TES using both electrical and mechanical responses, with a combination of experimental and simulated data. A new tool for modeling electrical stimulation (Mesin and Merletti 2008) is used to estimate the current field induced by

TES in the muscle. The activation of each MU is based on such a current distribution and on the excitation thresholds of the considered MU. Thus, MUs were recruited depending on their geometrical position and on the current density induced in their territory. Such a current is a function of distance from the stimulation point, thickness and conductivity of different tissue layers.

5 Exerted force corresponding to different stimulation currents was also simulated. Electrical and mechanical responses were compared with those recorded during TES of tibialis anterior (TA). The comparison of simulated and experimental electrically evoked contractions was aimed to understanding the relation between the recorded electrical / mechanical responses and the MU recruitment pattern during TES.

10

## **2. METHODS**

The experimental procedure and the simulation model are described in the following.

### **2.1 Experimental data collection and processing**

#### **15 2.1.1 Subjects**

Eight male subjects (mean  $\pm$  standard deviation: age  $26.6 \pm 3.6$  years; height  $174 \pm 7.6$  cm; weight  $71.5 \pm 9.1$  kg) volunteered to participate in the study. All subjects reported having no known neuromuscular or skeletal impairment. They were asked to refrain from performing any strenuous physical activity for 24 h before each measurement. Each subject received a detailed explanation of the study and gave written informed consent prior to participation. The study conformed to the guidelines in the Declaration of Helsinki and was approved by the Regional Ethics Committee.

20

#### **2.1.2 Surface EMG recording and stimulation technique**

Surface EMG signals were detected with a linear adhesive array (SPES Medica, Battipaglia, Italy) of eight electrodes with 5 mm interelectrode distance in single differential configuration during electrically elicited contractions. The EMG signals were amplified (EMG 16, 16 channel amplifier,

25

OT Bioelettronica, Torino, Italy), bandpass filtered (3-dB bandwidth, 10–500 Hz), sampled at 2048 samples/s per channel, displayed in real time, and converted into digital data by a 12-bit acquisition board. The stimulator triggered acquisition of the M-waves so that subsequent M-waves could be averaged. The part of the skin where the optimal location for the array was identified was treated  
5 with abrasive paste (Every, Spes Medica, Battipaglia, Italy). To assure proper electrode-skin contact, 20  $\mu$ l of conductive gel was inserted into the electrode cavities of the array with a gel dispenser (Multipette Plus, Eppendorf AG, Hamburg, Germany).

Stimulation was provided by a neuromuscular stimulator (DEM, Torino, Italy) equipped with a hybrid output stage (Knaflitz and Merletti, 1988). An adhesive stimulation electrode (SPES Medica,  
10 Battipaglia, Italy; size 35 x 45 mm, reduced in dimensions to 30 x 30 mm for the purposes of the study) was placed over the muscle under study while a large electrode (size 100 x 130 mm) was placed over the antagonist muscle to close the stimulation current loop (monopolar stimulation), as previously described (Mandrile et al 2003).

The stimulation current pulse was a symmetric biphasic square wave of 200  $\mu$ s duration at 20 Hz.

15

### 2.1.3 Experimental procedure

The TA muscle of the dominant side (the right for all subjects) was investigated. The right leg of the subjects was placed in an isometric brace (Orizio et al 2004) and the foot was fixed to a wooden plate at 120° (180° being full extension of the foot, see Figure 1A). A load cell fixed to the wooden  
20 plate measured the force generated during the contractions. Before placement of the stimulation electrode, all the motor points of the investigated muscle were identified by stimulating the muscle at increasing currents, with a frequency of 2 Hz, using a symmetric biphasic square current waveform with duration of 200  $\mu$ s applied with a pen electrode with 1 cm<sup>2</sup> surface. All the motor points were marked on the skin. The motor point chosen for the stimulation was always the most  
25 distal one, in accordance with Roy et al. 1986, Knaflitz et al. 1990, Farina et al. 2004a.

The surface array for EMG detection was located between the stimulation electrode and the distal tendon, and was aligned to the direction of the muscle fibers. The most proximal electrode of the array for EMG detection was 25 mm from the centre of the stimulation electrode.

**Figure 1 about here**

5 Biphasic constant level stimulation currents at 20 Hz were applied in different stimulation sessions for 3 s, separated by 1 minute rest (see Figure 1B). The amplitude of the stimulation current increased in subsequent sessions by steps of 1.7 mA and ranged between a minimum of 17 mA and the maximum intensity tolerated by the subject.

Moreover, an additional four electrode array was placed over the extensor digitorum longus muscle, 10 an agonist of the TA muscle, to evaluate possible activation of agonist muscles at high stimulation levels.

The experimental setup for isometric measurement of the force produced by the TA muscle during electrical stimulation is shown in Figure 1A. The stimulation protocol is shown in Figure 1B.

15 **2.2 Simulation model**

**2.2.1 Mathematical model of stimulated current distribution**

The mathematical model of current distribution is the following (Mesin and Merletti 2008)

$$\nabla \cdot J = -\nabla \cdot \left[ \left( \underline{\underline{\sigma}} + \varepsilon_0 \varepsilon_r \frac{\partial}{\partial t} \right) \nabla \varphi \right] = I \quad (1)$$

where  $\varphi$  is the electric potential (V) in space,  $J$  is the current density in the medium ( $A/m^2$ ),  $I$  is 20 the source current density ( $A/m^3$ ),  $\underline{\underline{\sigma}}$  is the conductivity tensor (S/m),  $\varepsilon_0 = 8.854 \times 10^{-12}$  F/m is the permittivity of the vacuum and  $\varepsilon_r$  is the relative permittivity of the biological tissue considered. A plane layer model was considered (see Figure 2A), with insulation conditions at the surface. Skin (1 mm thick), fat (thickness in the range 2-8 mm), and muscle (extending to infinity) tissues were considered. Interface conditions were the continuity of the potential and of the current flux.



Conductivity and permittivity are frequency dependent in biological tissues (dispersion; Stoykov et al 2002). Data provided in (Gabriel et al 1996) (which include dispersion) were used. The simple assumptions for the geometry allow obtaining an analytical solution in the Fourier transform domain (Mesin and Merletti 2008). The solution in time and space was obtained by numerical inversion of the sampled temporal and spatial frequencies. Time sampling frequency was  $2^{15} \cong 32 \text{ kHz}$ , and 256 samples were considered (which corresponds to a temporal interval of about 8 ms). The space variables  $x, z$  were sampled with step  $\Delta x = 4 \text{ mm}$ , 64 samples (which corresponds to a square domain with 256 mm side). This sampling allowed low aliasing and tail truncation of the spatial transfer function.

10

### 2.2.2 Stimulation of muscle fibers

The current distribution was calculated by time convolution of the impulse response and the stimulation current waveform. It was computed on the plane under the stimulation site perpendicular to the fiber direction (referred to as plane of stimulation, Figure 2, A1).

15 It was assumed that all end-plates were located in the plane of stimulation. It was further assumed that the current induced within the muscle stimulates the terminal branches of motor neurons close to the end-plates. The excitation of the MUs was based only on the local current density in the plane of stimulation. The terminal branches were assumed to be parallel to the muscle fibers in the plane of stimulation. As the current density in the plane of stimulation is orthogonal to the muscle fibers (and hence also to the terminal branches, under our assumptions), this current flows through the excitable membranes of the terminal branches of the motor neurons, determining a change of transmembrane potential. A simple RC model of membrane (considering only the transmembrane resistivity and permittivity) was used for the estimation of the stimulation induced change of the transmembrane potential. The impulse response of the membrane is a decaying exponential with  
20  
25 characteristic time of the order of 1 ms ( $C = 1 \mu\text{F}/\text{cm}^2$ ,  $R = 1 \text{ k}\Omega\text{cm}^2$ ; Cartee and Plonsery 1992).

The transmembrane potential was obtained in each point of the plane of stimulation as a time convolution of the current density with the impulse response of the membrane.

A terminal branch of a motor neuron (and then a MU) is excited if the transmembrane potential is higher than a threshold. The level of excitability is higher for large fibers (which means they have lower thresholds) than for small ones. Assuming a relation of proportionality between dimension of terminal branches of motor neurons and excitability threshold, a maximal variability of 100% in the values of the thresholds can be predicted (Prakash and Sieck 1998; Reilly 1992).

Different assumptions on the excitability were tested:

- 1) No relation between excitability threshold and MU dimension (MU thresholds chosen randomly, with uniform distribution).
- 2) Excitability threshold larger for larger MUs.
- 3) Excitability threshold smaller for larger MUs.

In all cases the excitability thresholds were scaled in order to take values between 1 and 2 (with 1 corresponding to the minimum level of simulated stimulation current, which elicited only one MU).

**Figure 2 about here**

### 2.2.3 Model of generation of EMG signals

The plane layer model of generation of surface EMG signals proposed in (Farina and Merletti 2001) was considered to simulate motor unit action potentials (MUAP). Only the conductivity of the tissues was considered (values provided in (Gabriel et al 1996) evaluated at frequency 100 Hz), neglecting permittivity. The transmembrane current was modeled as the second spatial derivative of the transmembrane potential, mathematically described in (Rosenfalk 1969). Finite length fibers (160 mm long) symmetrical with respect to the neuromuscular junction were simulated with density of one fiber per  $4 \text{ mm}^2$ , considering generation, propagation and extinction of the current density source. Each single fiber action potential (SFAP) was used to simulate a MUAP, with an amplitude scaling factor proportional to the number of fibers belonging to the MU. Such MUAP was then

filtered to approximate the smoothing due to the spread of the neuromuscular junction and tendon endings (8 mm) by a time convolution with a Gaussian function (with standard deviation equal to one fourth of the time taken by the intracellular potential to cover a distance equal to the spread of the neuromuscular junction and tendon endings). In this way, each simulated fiber was considered  
 5 as representative of a MU.

The number of fibers in the MUs was distributed as an exponential function (Enoka and Fuglevand 2001), with the largest MU including a number of fibers 20 times larger than that of the smallest MU. Higher values of CV were associated to larger MUs (Andreassen and Arendt-Nielsen 1987).

Different distributions of CV (with same range 3-5 m/s) and spatial distributions of the MUs within  
 10 the muscle were simulated:

- 1) Uniform spatial distribution of the MUs within the muscle; Gaussian CV distribution with mean 4 m/s and standard deviation 0.4 m/s.
- 2) Larger MUs deeper in the muscle; Gaussian CV distribution with mean CV varying linearly between 3.5 and 4.5 m/s as a function of the depth within the muscle and standard deviation 0.2 m/s.
- 15 3) Larger MUs more superficial; Gaussian CV distribution with mean CV varying linearly between 4.5 and 3.5 m/s as a function of the depth within the muscle and standard deviation 0.2 m/s.

The M-wave was simulated by a synchronous sum of all MUAPs corresponding to the MUs which were estimated to be excited, using the stimulation model described in the previous section (see Figure 2, A2).

20

#### 2.2.4 Isometric force model

The isometric force model for MUs described in (Fuglevand et al 1993) was used to simulate the twitch force of each elicited MU. Specifically, 1) the peak twitch force  $PF_n$  of the  $n^{\text{th}}$  MU was defined as

25

$$PF_n = RP^{n/N} \quad (2)$$

where  $N$  is the total number of MUs and  $RP$  is the ratio between the maximum and the minimum peak twitch force (assumed to be 100 in this study); 2) contraction time  $T_n$  of the  $n^{\text{th}}$  MU was given by

$$T_n = \frac{T_L}{PF_n^{1/c}} \quad (3)$$

5 where  $T_L = 90 \text{ ms}$  and  $c = \log_{RT} RP$ , where the base of the logarithm is the range of contraction times assumed to be  $RT=3$  (with this choice of the parameters  $T_L$  and  $RT$ , contraction times defined in Eq. (3) varied between the largest value corresponding to the smallest MU for which  $T_1 = T_L = 90 \text{ ms}$  and the lowest value, corresponding to the largest MU, for which  $T_N = T_L / RP = 30 \text{ ms}$ ); 3) a non-linear (sigmoid) relation between force and stimulus rate as  
 10 described in (Fuglevand et al 1993) was finally included in the model introducing a gain factor  $g_n$  depending on the  $n^{\text{th}}$  MU considered and on the firing frequency. The expression of the time evolution of the single force twitch was

$$f(t) = g_n \frac{PF_n t}{T_n} e^{1-(t/T_n)} . \quad (4)$$

The total force was obtained as a sum of the twitch forces of each elicited MU (see Figure 2 B).

15

## 2.3 Processing

### 2.3.1 Preliminary processing of the experimental data

The variables considered to investigate muscle contraction at different stimulation amplitudes are average rectified value (ARV), mean frequency (MNF), conduction velocity (CV) estimated from  
 20 M-waves and force level (Figure 2 B).

For each stimulation level, the 40 M-waves (60 responses excluding those during the first second of stimulation) of each channel were aligned and averaged to compute the mean M-wave for each channel. Only stimulation levels eliciting an M-wave were considered (discarding the first levels for

which no electrical response was obtained). The ARV and the MNF were estimated as an average obtained from the four mean M-waves of the four central single differential channels of the electrode array over a time window of 25 ms where the stimulation artifact was not present (zero padding was used to interpolate the frequency resolution to 1 Hz). The estimation of muscle fiber CV was computed using a maximum likelihood approach on the four consecutive selected single differential channels (Farina et al 2001).

For each stimulation train, the value of the force was averaged during the second half of the first second of stimulation (Figure 3B). This time window was selected to discard both the initial transient and the progressive increase of force induced in some subjects by the twitch potentiation after the first second of stimulation.

### 2.3.2 Data post-processing

Different ranges of stimulation current and values of force and EMG variables were associated to different subjects and simulations. In order to compare experimental data from different subjects and simulation sets, both the stimulation current and the values of the force or EMG variables were rescaled using the normalization procedure described below.

The curve of ARV vs stimulation current level showed a knee (i.e. a point of maximum curvature), separating a region of increase of M-wave amplitude (for low current intensities) from a plateau (for higher current intensities, as shown in Figure 3C). The current intensity corresponding to the knee can be considered as the maximal stimulation level. Supramaximal current is obtained by increasing further the stimulation level. We considered current levels up to the intensity corresponding to 130% of the knee. This value never exceeded the maximum tolerable stimulation amplitude for any subject. The axis of the stimulation current was scaled imposing zero value to the minimum stimulation level and unitary value to the current at which the knee appeared. To estimate automatically the position of the knee, the following procedure was applied. Given a number  $N$  of stimulation steps, the first  $(N-M)$  values of ARV (with  $1 < M < N$ ) are interpolated by a line, the

remaining M values by another line. In this way, for each value of M, the ARV vs stimulation current curve is approximated by two lines (see Figure 3C). The value of M providing the minimum mean square error was identified as the current step corresponding to the knee of the ARV vs stimulation current curve.

5 Only values of force and EMG variables in the range [0, 1.3] of normalized stimulation current were considered for further processing. Stimulation current values were interpolated in order to have the same number of points of each curve associated to different subjects or simulations. Finally, force and EMG variables were normalized with respect to the value obtained at the maximum stimulation current considered (i.e., 130% of the knee current). By this procedure both  
10 the x-axis and the y-axis were normalized, obtaining the normalized stimulation current and the normalized quantity (force or EMG variable), respectively.

### 2.3.3 Statistical analysis

Analysis of variance (ANOVA) was applied to the simulated data. Significance level was set to  
15  $p < 0.01$ . Three factors were considered for the ANOVA: fat layer thickness, MU recruitment order, and type of MU distribution (random or larger MUs deeper/superficial). When ANOVA indicated significant variations, pair-wise comparisons were performed with post-hoc Student-Newman-Keuls (SNK) test, with significance level set to  $p < 0.01$ .

Wilcoxon signed rank test for zero median was applied to variables extracted from experimental  
20 signals to test if they were statistically different from zero.

Statistical analysis was performed with Statistica 6 for Windows (Statsoft Inc., Tulsa, OK) software package. All values are given as mean  $\pm$  standard deviation or mean  $\pm$  standard error, as indicated.

## 3. RESULTS

25 Figure 3 shows experimental M-waves, ARV and force with respect to stimulation amplitude of the TA muscle, during transcutaneous stimulation at different amplitudes in a representative subject. A

superimposition of single differential M-waves is shown in A). Force traces recorded during the first second of stimulation are shown in B). The curve ARV vs stimulation intensity is shown in C). Such a curve shows a saturation of EMG amplitude, with a knee which was used to normalize the current intensity, in order to compare data from different subjects (see Section 2.3.2). The curve of force vs stimulation amplitude is shown in D). Data are interpolated by a second order polynomial with upward concavity, which means that the leading coefficient (i.e. the coefficient of the second order term in a second order polynomial) was positive. No activity was detected from the electrodes placed over the extensor digitorum longus muscle (synergist of TA muscle) during the stimulation of the TA indicating that force is likely generated by TA only.

**Figure 3 about here**

10

Figure 4 shows ARV, MNF, CV and force values (curve of individual subjects and mean  $\pm$  standard deviation over the eight subjects) obtained from the experimental protocol. The values along the X axis are normalized with respect to the stimulation level corresponding to the knee of the ARV; those along the Y axis are normalized with respect to the values obtained at 130% of the current level corresponding to the knee. The mean slope of the curves of CV for increasing stimulation current and the mean leading coefficient of the second order polynomial interpolating the force curves were both positive. Nevertheless, Wilcoxon signed rank test indicated that only the CV slope was statistically higher than zero.

**Figure 4 about here**

Figure 5 shows the percentage variation of CV and MNF with respect to the initial value of the regression line and the leading coefficient of the second order polynomial interpolating the force curve from simulated signals. Results from simulations with different fat thicknesses, MU recruitments and MU distributions (mean  $\pm$  standard deviation) are shown in A). The dependence of CV percentage variation, MNF percentage variation and leading coefficient of force on MU recruitment and distribution is shown in B) (mean  $\pm$  standard error). No variable was statistically dependent on fat layer thickness. ANOVA indicated that each of the three variables investigated

20

25

(CV and MNF percentage variation, leading coefficient of force) was statistically dependent on MU distribution ( $F=275$ ,  $p<0.01$  for CV variation;  $F=189$ ,  $p<0.01$  for MNF variation;  $F=523$ ,  $p<0.01$  for leading coefficient of force) and MU recruitment order ( $F=8.62$ ,  $p<0.01$  for CV variation;  $F=39$ ,  $p<0.01$  for MNF variation;  $F=12$ ,  $p<0.01$  for leading coefficient of force). Post-hoc SNK test indicated that each investigated variable was statistically affected by different MU distributions ( $p<0.01$ ). Moreover, post-hoc SNK test disclosed pair-wise differences for each of the variables estimated with different MU recruitment orders ( $p<0.01$ ), with the exception of the following three cases: leading coefficient of force or percentage variations of MNF estimated in the case in which small MUs were assumed to have low recruitment thresholds or recruitment thresholds were assigned randomly; percentage variations of CV estimated in the case in which low thresholds were assumed to be associated to large MUs or recruitment thresholds were assigned randomly.

**Figure 5 about here**

#### **4. DISCUSSION**

TES was investigated in this work by experimental and simulated data. The combined analysis of electrical and mechanical information provided valuable insight into the MU recruitment during TES of the TA muscle.

##### **4.1 Experimental stimulated contractions**

*EMG results.* The leveling off of the EMG ARV/stimulation amplitude relationship suggests that, beyond a given level of injected current, the recruited MUs may be deeply located, providing a small contribution to the EMG signal. CV mostly increased for increasing amplitude of the stimulation current in the range 0.25 – 1.00 of the normalized stimulation amplitude. From cable theory (the larger is the cable, the faster is the propagation of action potentials), these findings may suggest that the diameter of the muscle fibers and the dimension of the MUs recruited for higher level of stimulation current is increasing. Another possible interpretation is that recruitment for increasing stimulation proceeds from superficial to deep MUs, with the latter contributing to biasing



CV estimation toward higher values due to the larger relative weight of non propagating components in the corresponding MUAPs. This behavior mirrored the ARV/stimulation amplitude relation. On the contrary the MNF/stimulation amplitude relationship did not follow the CV/ or ARV/stimulation amplitude pattern. This result may indicate that other phenomena, probably  
5 related to MUAP shape or MUs distribution within the muscle (as discussed in Section 4.2.3), may influence the EMG spectral features differently in different subjects.

*Force results.* As indicated in the Results section, contribution of TA synergists can be excluded during the considered stimulated contractions. On this basis, considering that the force output still increased while the EMG amplitude plateaued in the last part of their relationship with increasing  
10 stimulation amplitude, it can be concluded that beyond a given stimulation level, the recruitment of MUs deeply located does not substantially contribute to surface EMG, but still contribute to tension output.

#### **4.2 Model of simulation of electrically elicited contractions**

The model of simulation is based on a number of assumptions, which should be considered when  
15 comparing simulated data and real experiments. The most important approximations considered in the model are defined below:

1. The stimulation current was applied as a point source, whereas in experiments the stimulation electrode had a surface of 30 x 30 mm.
2. A simple plane layer model was used, neglecting the effects of the curvilinear geometry of a  
20 physiological tissue on the distribution of the current within the muscle and on the M-wave.
3. Neuromuscular junctions were assumed to be distributed in a plane under the stimulation electrode.
4. A linear model of the membrane was considered to determine if an axon fiber was excited  
by the current injected by the external generator.

25 These approximations were introduced to keep the model manageable while still describing the most important features of the real physiological problem. Thus, discrepancies between simulated

and experimental data are expected when considering specific simulations or experimental results. Nevertheless, indications extracted averaging many simulations are expected to be in line with those obtained averaging experimental data.

#### **4.3 Simulation fitting of the experimental data: possible role of MU recruitment order and geometrical distribution.**

Results concerning MU recruitment order during TES are controversial (Heyters et al 1994; Trimble and Enoka 1991; Feiereisen et al 1997; Knaflitz et al 1990). In all our simulations, MNF decreased with increasing amplitude of stimulation current and hence this variable did not help to discriminate neither between different MU recruitments nor spatial MU distributions. Thus, we'll focus on the other two investigated variables: CV variations with increasing stimulation current and leading coefficient of the second order approximation of the force vs stimulation curve.

The effect on the electrical and mechanical responses of assigning the excitation thresholds either randomly, or ordered according to MU dimension, or with the opposite order was found statistically significant in this study. More in detail, our results indicated that, increasing the stimulation current, the CV variations were higher when small MUs had lower thresholds than large MUs. On the contrary, the MNF variations and the leading coefficient of the force response were higher when larger MUs had lower thresholds than smaller MUs. Nevertheless, on the average, CV increased, MNF decreased, leading coefficient of the second order approximation of force curve was positive when increasing the injected current, regardless of whether the excitation thresholds were assumed to be higher for larger or smaller MUs (Figure 5B).

On the other hand, geometrical distribution of MUs (i.e., placing small/large MUs preferentially superficial/deep within the muscle) had a paramount role on electrical and mechanical responses. Moreover, the effect of the geometrical distribution of the MUs determined significant changes in the estimated variables when comparing any pair of the three simulated distributions (SNK test,  $p < 0.01$ ). In particular, if large MUs were assumed to be placed deep 1) the estimated CV increased for increasing stimulation current and 2) the leading coefficient of the second order approximation

of the curve associating force to stimulation current was positive. The increase of CV is interpreted as the effect of larger MUs recruited for greater current amplitudes. The positivity of the leading coefficient of the force curve is related to the low increase due to the stimulation of small MUs (recruited first as they were located close to the stimulation point) followed by a faster increase as the stimulation current is high enough to activate larger MUs (located far from the stimulation electrode). These findings are in line with experimental data.

## CONCLUSIONS

This study addresses the problem of MU recruitment during TES using both experimental and simulated data, and investigating information derived from both electrical and mechanical responses. Two variables, observed with increasing current level, reflect the order of recruitment and the spatial distribution of the MUs: 1) CV obtained from the electrical response and 2) leading coefficient of the second order polynomial interpolating the mechanical response (on the other hand, spectral variables appear to be particularly sensitive to inter-individual variability). These variables were positive for the experimental data and for the simulated data only if larger MUs were assumed to be preferentially deep within the muscle, regardless of either the distribution of excitation thresholds or fat layer thickness.

Two conclusions are provided comparing our simulations to experiments:

1) Larger MUs are preferentially distributed deep in the TA muscle (even though large individual differences are evident), in line with a histochemical study (Henriksson-Larsen et al 1985), indicating that fibers of TA muscle (which could be either of type I or type II) have larger diameters in the deep than in the superficial layers.

2) MUs are recruited following mainly a geometrical order (MUs closer to the stimulation electrode are recruited first), in line with a positron tomography study during electrically elicited contractions of quadriceps (Vanderthommen et al 1997) and with a previous work comparing simulated and experimental M-waves from biceps brachii (Farina et al 2004a), suggesting that MUs tended to be activated from low CV to high CV and from superficial to deep muscle layers when increasing the

intensity of TES. This finding provides an interpretation of the controversial results reported in the literature on MU recruitment during TES, since MU distribution may be different in different muscles (e.g. superficial MUs are larger than deep MUs in the vastus lateralis, Knight and Kamen, 2005) and can be affected by inter-individual variability.

5

### **Acknowledgements**

This study was supported by European Space Agency (Project MESM, contract nr: 15097/01/NL/SH), Italian Space Agency (Project OSMA, contract nr: I/007/06/0), Compagnia di San Paolo, and Fondazione CRT.

10

### **REFERENCES**

1. Andreassen S., Arendt-Nielsen L., Muscle fiber conduction velocity in motor units of the human anterior tibial muscle: A new size principle parameter, *J Physiol*, 1987. 391: 561-571.
2. Bajd T., Kralj A., Stefancic M., Lavrac N. Use of functional electrical stimulation in the lower extremities of incomplete spinal cord injured patients, *Artif Organs*. 1999. 23: 403-409.
3. Basmajian J.V., DeLuca C.J. *Muscle Alive: Their Functions Revealed by Electromyography*. Williams and Wilkins, Baltimore. 1985
4. Bigland-Ritchie B., Woods J.J. Changes in muscle contractile properties and neural control during human muscular fatigue, *Muscle Nerve*. 1984. 7(9): 691-699. Review.
5. Cartee LA, Plonsey R. The transient subthreshold response of spherical and cylindrical cell models to extracellular stimulation, *IEEE Trans Biomed Eng*. 1992. 39(1): 76-85.
6. Dimitrijevic MM, Dimitrijevic MR. Clinical elements for the neuromuscular stimulation and functional electrical stimulation protocols in the practice of neurorehabilitation. *Artif Organs*. 2002 Mar;26(3):256-9. Review.

20

7. Enoka RM. Neuromuscular electrical stimulation: what is activated? In: Biomedical engineering in exercise and sports, edited by Rainoldi A, Minetto MA, Merletti R. Torino, Italy: Edizioni Minerva Medica, 2006.
8. Enoka RM, Fuglevand AJ. Motor unit physiology: some unresolved issues, *Muscle Nerve*. 2001. 24: 4-17. Review.
9. Farina D, Merletti R. A novel approach for precise simulation of the EMG signal detected by surface electrodes, *IEEE Trans. Biomed. Eng.*, 2001. 48: 637-646.
10. Farina D., Muhammad W., Fortunato E., Meste O., Merletti R., Rix H. Estimation of single motor unit conduction velocity from surface electromyogram signals detected with linear electrode arrays, *Med. Biol. Eng. Comput.* 2001. 39: 225-236.
11. Farina D, Blanchietti A, Pozzo M, Merletti R. M-wave properties during progressive motor unit activation by transcutaneous stimulation, *J Appl Physiol* 2004a. 97: 545–555.
12. Farina D, Mesin L, Martina S, Merletti R. Comparison of spatial filter selectivity in surface myoelectric signal detection: influence of the volume conductor model, *Med Biol Eng Comput.* 2004b. 42(1): 114-120.
13. Feiereisen P, Duchateau J, Hainaut K. Motor unit recruitment order during voluntary and electrically induced contractions in the tibialis anterior, *Exp Brain Res*. 1997. 114: 117-123.
14. Fuglevand A.J., Winter D.A., Patla A.E. Models of recruitment and rate coding organization in motor-unit pools, *J Neurophysiol*. 1993. 70: 2470-2488.
15. Gabriel S, Lau RW, Gabriel C. The dielectric properties of biological tissues: II. Measurements in the frequency range 10 Hz to 20 GHz, *Phys Med Biol*. 1996. 41(11): 2251-2269.
16. Gielen FL, Wallinga-de Jonge W, Boon KL. Electrical conductivity of skeletal muscle tissue: experimental results from different muscles in vivo, *Med. Biol. Eng. Comput.* 1984. 22(6): 569-577.
17. Gorman PH, Mortimer JT. The effect of stimulus parameters on the recruitment characteristics of direct nerve stimulation, *IEEE Trans Biomed Eng.* 1983. 30: 407-414.

18. Heyters M, Carpentier A, Duchateau J, Hainaut K. Twitch analysis as an approach to motor unit activation during electrical stimulation, *Can J Appl Physiol*. 1994. 19: 451-461.
19. Henriksson-Larsen K, Friden J, and Wretling ML. Distribution of fiber sizes in human skeletal muscle. An enzyme histochemical study in m tibialis anterior, *Acta Physiol Scand*. 1985. 123: 171–177.
20. Knaflitz M, Merletti R. Suppression of simulation artifacts from myoelectric-evoked potential recordings. *IEEE Trans Biomed Eng*. 1988. 35(9): 758-763.
21. Knaflitz M, Merletti R, De Luca CJ. Inference of motor unit recruitment order in voluntary and electrically elicited contractions, *J Appl Physiol*. 1990. 68: 1657-1667.
22. Knight CA, Kamen G. Superficial motor units are larger than deeper motor units in human vastus lateralis muscle. *Muscle Nerve*. 2005. 31(4): 475-480.
23. Kuhn A, Keller T, Lawrence M, Morari M. A model for transcutaneous current stimulation: simulations and experiments, *Med Biol Eng Comput*. 2009. 47(3): 279-289.
24. Lawrence JH, De Luca CJ. Myoelectric signal versus force relationship in different human muscles, *J Appl Physiol*. 1983. 54(6): 1653-1659.
25. Lee J, Adam A, De Luca CJ. A simulation study for a surface EMG sensor that detects distinguishable motor unit action potentials, *J Neurosci Methods*. 2008. 15; 168(1): 54-63.
26. Mandrile F, Farina D, Pozzo M, Merletti R. Stimulation artifact in surface EMG signal: effect of the stimulation waveform, detection system, and current amplitude using hybrid stimulation technique, *IEEE Trans Neural Syst Rehabil Eng*. 2003. 11: 407–415.
27. Mayr W, Bijak M, Girsch W, Hofer C, Lanmuller H, Rafolt D, Rakos M, Sauermann S, Schmutterer C, Schnetz G, Unger E, Freilinger G. MYOSTIM-FES to prevent muscle atrophy in microgravity and bed rest: preliminary report, *Artif. Organs*. 1999. 23(5): 428-431.
28. Merletti R, Knaflitz M, De Luca CJ. Myoelectric manifestations of fatigue in voluntary and electrically elicited contractions, *J Appl Physiol*. 1990. 69: 1810–1820.

29. Merletti R, De Luca CJ, Sathyan D. Electrically evoked myoelectric signals in back muscles: effect of side dominance, *J Appl Physiol*. 1994. 77(5): 2104-2114.
30. Merletti R, Parker P. *Electromyography: physiology, engineering and non-invasive applications*, IEEE Press and John Wiley, pp. 97-100, 2004.
- 5 31. Mesin L, Merletti R. Distribution of electrical stimulation current in a planar multi layer anisotropic medium, *IEEE Trans. on Biomed. Eng.* 2008. 55(2): 660 – 670.
32. Orizio C, Gobbo M, Diemont B. Changes of the force-frequency relationship in human tibialis anterior at fatigue, *J. Electromyogr. Kinesiol*, 2004. 14: 523-530.
33. Prakash YS, Sieck GC. Age-related remodeling of neuromuscular junctions on type-  
10 identified diaphragm fibers, *Muscle Nerve*. 1998. 21(7): 887-895.
34. Reilly JP. *Electrical Stimulation and Electropathology*, Cambridge University Press, 1992.
35. Rosenfalck P. Intra and extracellular fields of active nerve and muscle fibers. A physico-mathematical analysis of different models, *Acta Physiol. Scand.* 1969. 321: 1-49.
36. Roy SH, De Luca CJ, Schneider J. Effects of electrode location on myoelectric conduction  
15 velocity and median frequency estimates. *J Appl Physiol*. 1986. 61(4): 1510-1517.
37. Sadowsky CL. Electrical stimulation in spinal cord injury, *NeuroRehabilitation*, 2001. 16(3): 165-169.
38. Skold C, Lonn L, Harms-Ringdahl K, Hultling C, Levi R, Nash M, Seiger A. Effects of functional electrical stimulation training for six months on body composition and spasticity in  
20 motor complete tetraplegic spinal cord-injured individuals, *J. Rehabil. Med.* 2002. 34(1): 25-32.
39. Solomonow M, Baratta R, Shoji H, D'Ambrosia RD. The myoelectric signal of electrically stimulated muscle during recruitment: an inherent feedback parameter for a closed-loop control scheme, *IEEE Trans Biomed Eng.* 1986. 33: 735-745.
40. Stoykov NS, Lowery MM, Taflove A, Kuiken TA. Frequency- and time-domain FEM  
25 models of EMG: capacitive effects and aspects of dispersion, *IEEE Trans. on Biomed. Eng.* 2002 49(8): 763 – 772.

41. Trimble MH, Enoka RM. Mechanisms underlying the training effects associated with neuromuscular electrical stimulation, *Phys Ther.* 1991. 71: 273-280.
42. Vanderthommen M, Depresseux JC, Bauvir P, Degueldre C, Delfiore G, Peters JM, Sluse F, Crielaard JM. A positron emission tomography study of voluntarily and electrically contracted  
5 human quadriceps, *Muscle Nerve.* 1997. 20: 505-507.



## FIGURE CAPTIONS

**Figure 1.** A) Schematic drawing of the ergometer for isometric measurement of the force produced by the tibialis anterior muscle during electrical stimulation. B) Representation of the stimulation sequence used during the protocol.

5 **Figure 2.** A) Plane layer model, with indication of the detection system and of the different layer thicknesses considered. The plane of stimulation is shown in A1. This is the plane under the stimulation site, in which the current density is simulated to determine the MUs excited by the stimulation. Three representative examples of simulated M-waves corresponding to three levels of stimulation current are shown in A2. B) Results of the processing of signals for a representative  
10 simulation. Force level, mean frequency (MNF), average rectified value (ARV), and estimated conduction velocity (CV) are given for different percentages of the maximum simulated level of stimulation current.

**Figure 3.** M-wave, ARV and force versus stimulation amplitude of tibialis anterior muscle, during transcutaneous stimulation at different amplitude levels in a representative subject.

15 A) Superimposition of single differential M-waves obtained from a linear array of eight electrodes aligned to the muscle fibers. B) Superimposition of force traces during the first second of stimulation at increasing amplitude. C) ARV vs stimulation intensity showing a saturation of EMG amplitude; the current eliciting a just detectable M-wave and that corresponding to the knee were used to normalize the scale between 0 and 1, in order to compare data from different subjects. D)  
20 Force vs stimulation amplitude showing a higher contribution of the deeper motor units activated by the higher current levels.

**Figure 4.** ARV, MNF, CV and force values obtained from the experimental protocol (individual curves and mean  $\pm$  standard deviation over eight subjects). The values are normalized along the X axis as described in Fig. 3 and along the Y axis by the values obtained at 130% of the current level  
25 corresponding to the knee.

**Figure 5.** Percentage variation of CV and MNF with respect to the initial value of the regression line and leading coefficient of the second order polynomial fit of the force curve. A) Results from simulations with different MU recruitment and distribution (mean  $\pm$  standard deviation over 120 simulations). B) Average results showing the dependence on MU recruitment and distribution (mean  $\pm$  standard error). Pair-wise comparisons for which post-hoc Student-Newman-Keuls test disclosed statistically significant differences are indicated by asterisks.

Figure 1

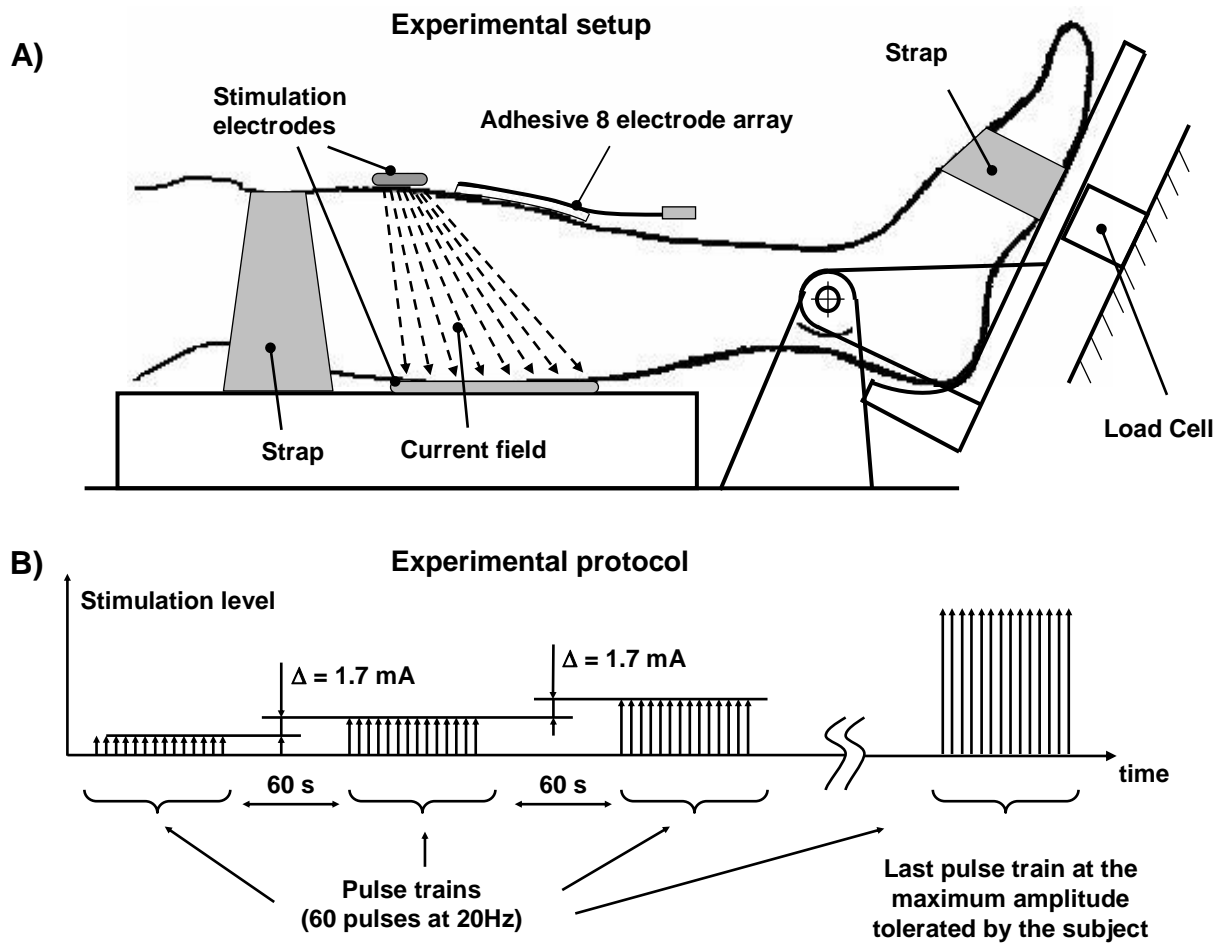


Figure 2

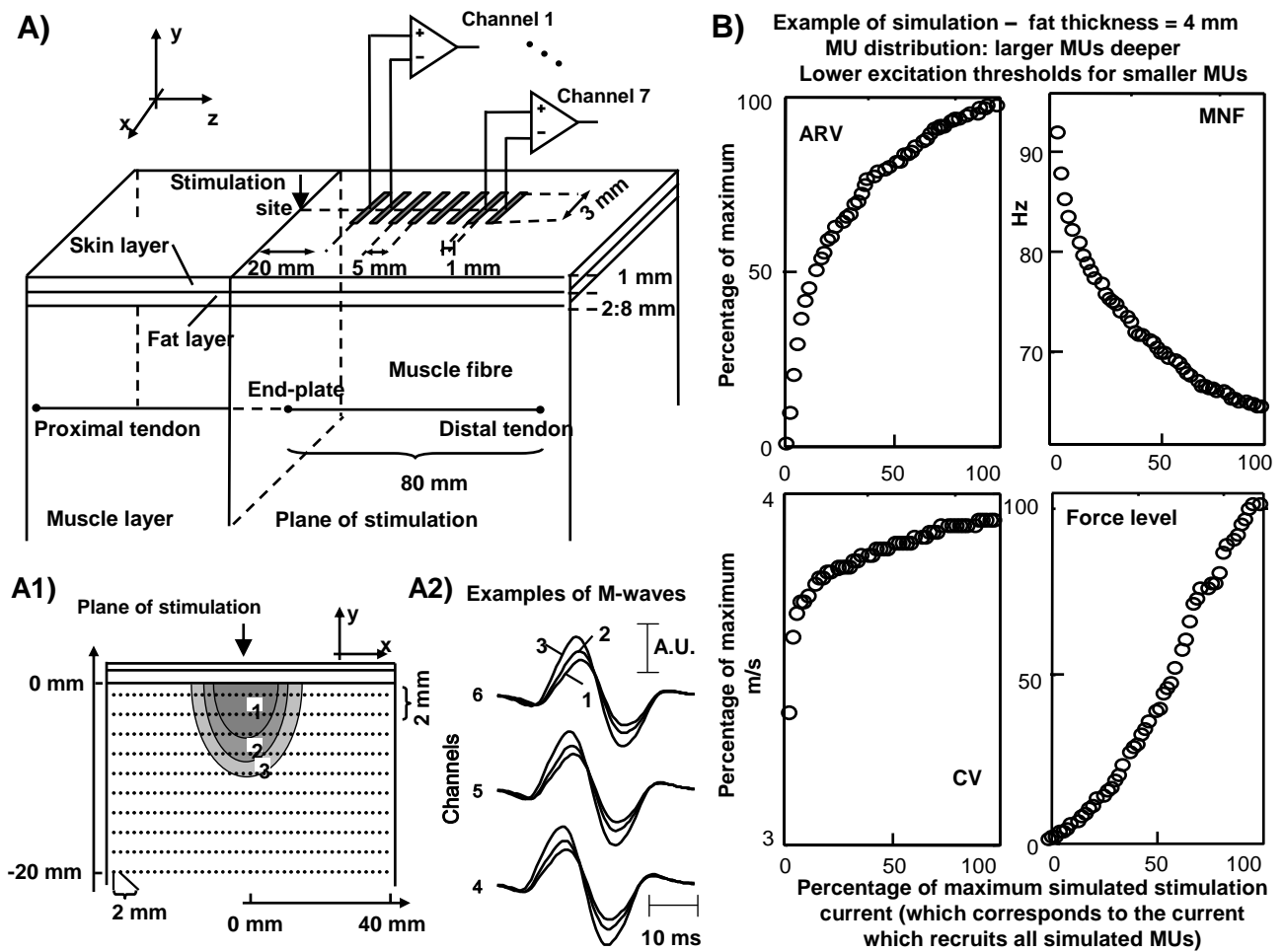


Figure 3

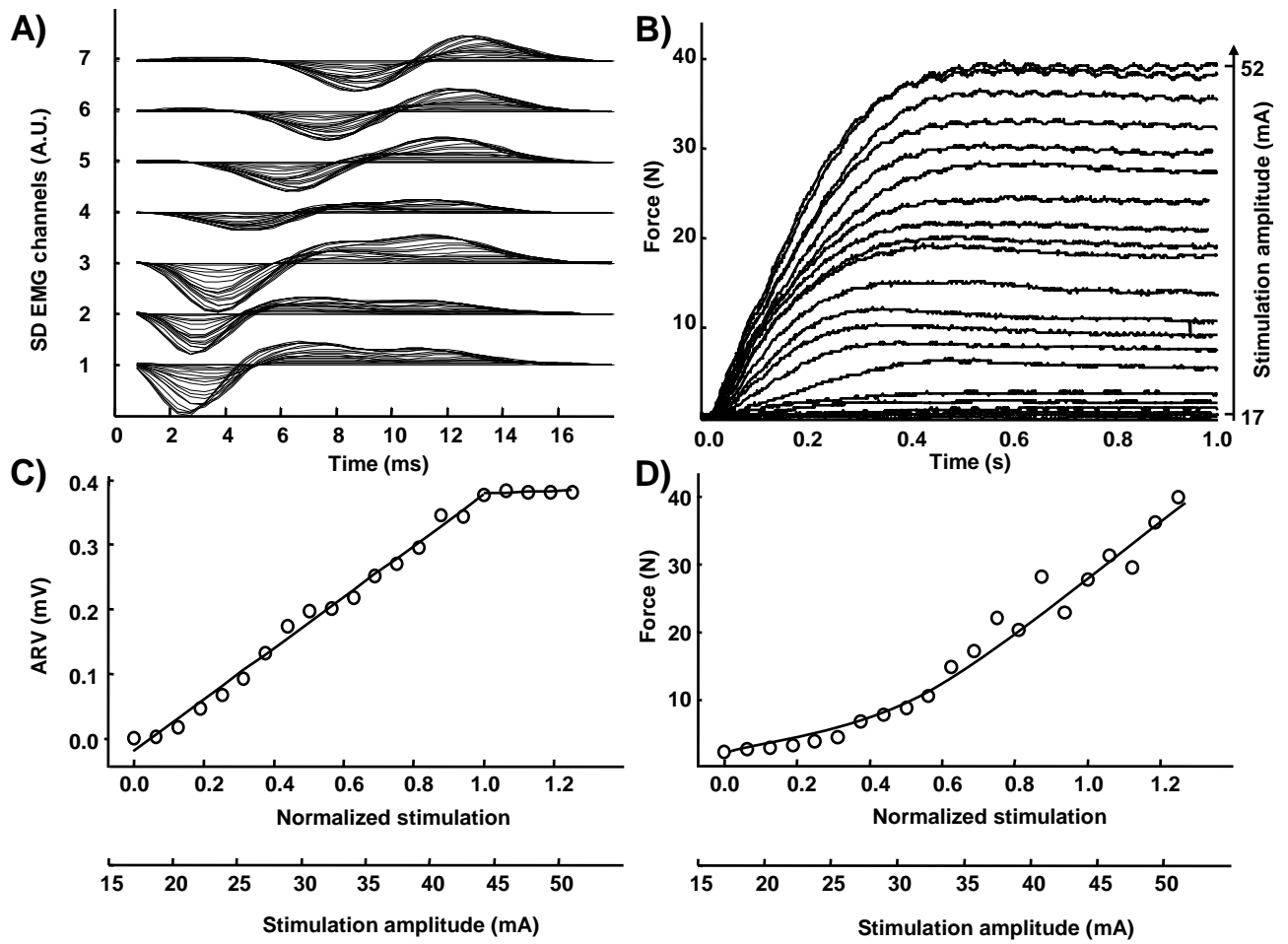


Figure 4

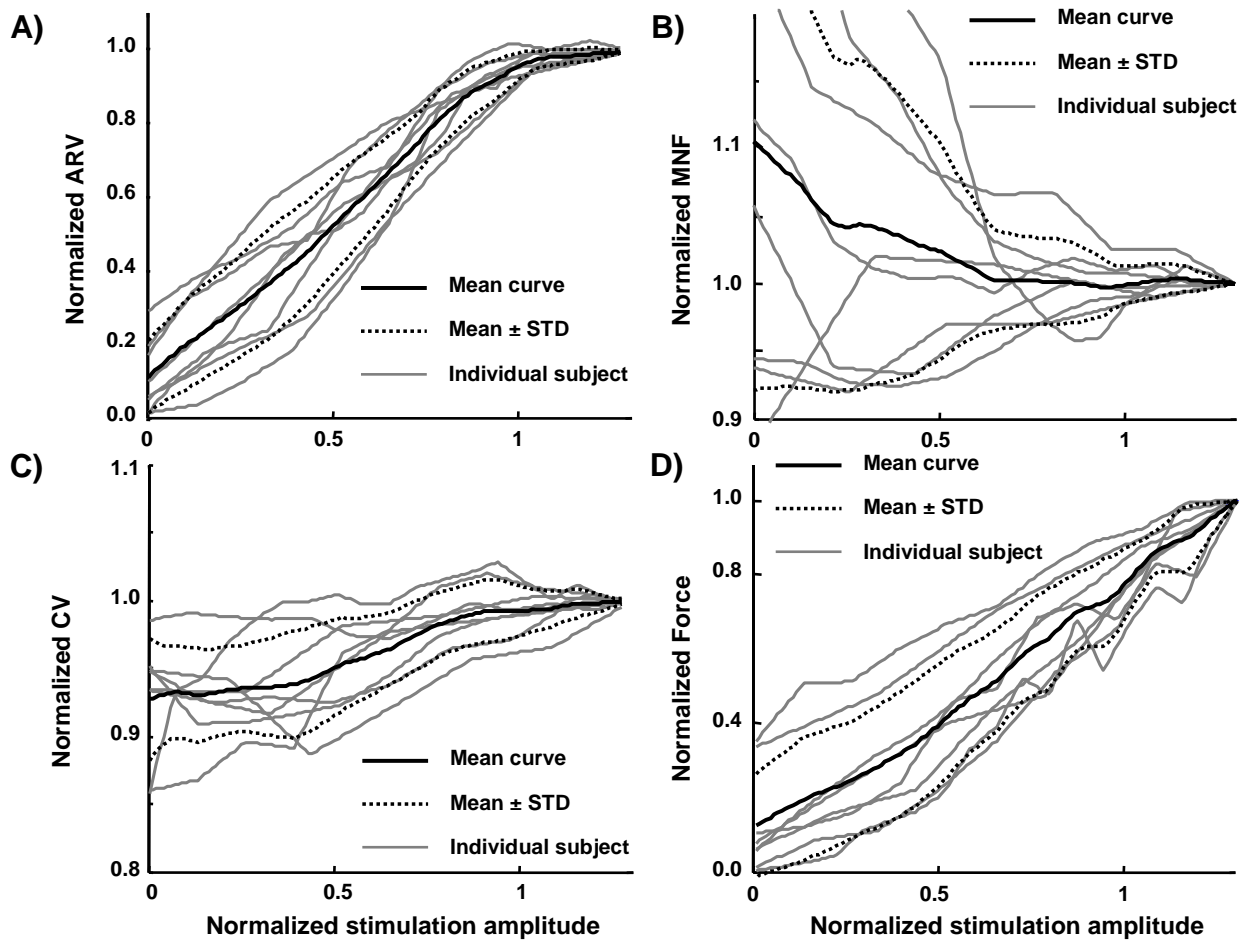


Figure 5

